Stress transfer at the interface of bonded joints between FRP and calcarenite natural stone

M. Accardi & L. La Mendola
Department of Structural and Geotechnical Engineering, University of Palermo, Italy

ABSTRACT: The reinforcing technique consisting of fiber reinforced polymer (FRP) sheets bonded to structural elements strongly depends on the effectiveness of the connection of the joints. With reference to calcarenite stone, which is one of the natural stones most employed in masonry constructions in the Mediterranean area, the paper aims to understand the stress transfer mechanism between calcarenite ashlar and reinforcing package consisting of carbon fiber reinforced polymer (CFRP) sheets impregnated with epoxy resin. For this purpose an experimental investigation is carried out on double-lap shear tests. The phenomenon of force transfer will be explained by placing strain-gauges along the CFRP bond length on the outside. The experimental investigation presented here refers to specimens with different CFRP bond length, 150, 100 and 50 mm, and it is addressed to extend the existing design models predicting the load-carrying capacity and the minimum transfer length to this kind of natural stone.

1 INTRODUCTION

Fiber reinforced composites with polymeric matrix are frequently used for the strengthening and rehabilitation of concrete structures; in particular, flexural and shear FRP reinforcing elements, externally bonded to reinforced concrete beams, constitute the larger body of the present-day applications.

Recently, the use of these materials has encouraged investigations on their applications to masonry structures, especially with reference to the large amount of historical masonry buildings in Europe and in particular in Italy. The use of FRP sheets or strips, instead of traditional materials or techniques, in order to strengthening structural masonry elements such as arches or vaults and masonry panels offers several advantages. The fundamental properties of this technique consist in the high strength, lightness, resistance to corrosion, easiness of application and possibility of removal.

In this context, a pressing need is felt for standard codes addressed to furnishing design procedures; while some code recommendations have been issued by the United States, Canada and the European Community (fib Bulletin 14) for reinforced concrete structures, not much has been done for masonry structures.

Therefore, a lot of scientific investigations have been published in this field on the experimental behavior of structural masonry elements strengthened with FRP (Eshani et al. 1999, Faccio & Foraboschi 2000, Como et al. 2000, Valluzzi et al. 2001) and analytical approaches have been proposed (Luciano & Sacco 1998, Briccoli Bati & Rovero 2000, Triantafillou 1998).

A rigorous formulation for structural masonry elements strengthened with FRP has been presented by Triantofillou (1998), who only considers the compression failure of masonry elements or tensile failure of FRP reinforcement, neglecting the bond failure mechanism. The latter is the most common mechanism of failure that can take place with a rapid diffusion process, especially in anchorages bonded with an epoxy resin to the matrix surface.

For this reason with reference to calcarenite stone, which is one of the natural stone most employed in masonry constructions in the Mediterranean area, an experimental investigation has been made to verify the extension of the existing design models, relative to concrete structures, also for this kind of natural stone. Calcarenite stone is made up mostly of microlamellibranchi and foraminifera calcareous shells in which the carbonaceous cement occludes partially the intergranular space and can be considered similar to concrete. It has different physical and mechanical properties in relation to its structure, porosity and texture, and can appreciably change even in the same quarry.

In the present research double shear pulling tests were carried out on calcarenite stone, also deducing the compressive and tensile strength for the same specimens as used for the bond tests. It was possible to compare the experimental results with the existing design models. The model proposed by Chen & Teng

(2001) was chosen for its effectiveness and simplicity in use for real applications.

2 LOAD-CARRYING CAPACITY

In the last few years several experimental investigations and analytical models have been proposed to predict the bond strength and the bond length for FRP externally bonded to concrete materials.

Different test methods (single or double shear pulling test, single or double shear pushing test and beam test) have been suggested with the aim of knowing the behavior of the connection between the reinforcement and the material where FRP has been applied, called the matrix (Horiguchi & Saeki 1997). These tests have been made on a single or double block reinforced with FRP; the methods are representative of different interfacial transfer mechanisms in structural elements.

To identify the parameters that govern the bond phenomenon, two basically different approaches have been used: the *stress approach*, in which the criterion for growth of the debonded FRP-matrix interface is expressed in terms of the interfacial bond stresses; and the *fracture mechanics approach*, in which the criterion for interfacial debonding is expressed in terms of energy balance.

Both approaches use the same following assumptions to study the FRP-matrix sub-system:

- the matrix and the fibers are homogenous, isotropic and linear elastic;
- the adhesive is only exposed to shear force;
- the adherents are in a state of pure tension, with no bending or shear effects.

These assumptions make it possible effectively to represent the actual behavior of the connection close to the discontinuity or cracked sections, where the bond failure is the delamination of the reinforcement from the matrix. Nevertheless, for other failure mechanisms, like peeling or ripping off, we must take shear and flexural effects on the reinforcement into account.

2.1 *Analytical approaches*

The stress approach for debonding is based on the assumption that debonding only takes place when the maximum bond stress τ at the interface reaches the threshold value.

Based on the assumptions given previously and writing the equilibrium condition and the compatibility for the two adherents it is possible to obtain the following differential equation that governs the interfacial behavior (Ottosen & Olsson 1988):

$$s'' - \frac{1+\lambda}{E_f \cdot t_f}\tau(s) = 0 \qquad (1)$$

where s = slip between fiber and matrix; E_f = Young modulus of fiber; t_f = thickness of the fiber; $\lambda = E_f A_f /(EA)$ axial stiffness ratio of the two adherents.

The general differential Equation (1) can be solved, in closed form, for different local bond constitutive laws $\tau = f(s)$: *cut-off type* (Volkersen 1938), *nonlinear type* (Pichler 1993) and *bilinear type with linear softening* (Ottosen & Olsson 1988, Wu & Niu 2002).

For the latter case:

$$\tau(s) = \begin{cases} \dfrac{G_{ep}}{t_{ep}} s & 0 \le s \le s_1 \qquad (2a) \\ \dfrac{G_{ep}}{t_{ep}} \dfrac{s_1}{(s_0 - s_1)} \cdot (s_0 - s) & s_1 < s \le s_0 \qquad (2b) \\ 0 & s > s_0 \qquad (2c) \end{cases}$$

where G_{ep} = shear modulus of epoxy resin; t_{ep} = thickness of epoxy resin; s_1 = maximum slip of ascending branch and s_0 = ultimate slip of descending branch. By introducing Equation (2) in Equation (1) and by solving the differential equation, it is possible to obtain the expression of the maximum load related to the minimum transfer length or a greater length:

$$F_{max} = b_f \sqrt{E_f \cdot t_f \cdot \tau \cdot s_0 (1+\lambda)} \qquad (3)$$

where τ = bond stress threshold value for the connection, b_f = width of the reinforcement. The shear threshold τ and ultimate slip s_0 values can be correlated with the matrix properties when the failure mechanism starts and propagates only inside the matrix. The expression in Equation (3) can be obtained by using the fracture mechanics approach. It is characterized by the assumption that the propagation of the debonding zone takes place when the energy release rate reaches a critical value, a value that is related to the fracture work of the interface FRP-matrix. When the debonded length increases in size, on the basis of the knowledge of the elastic energy stored in the structure, for overlap joints it is possible to obtain an expression relating the external load F with the interfacial fracture energy G. For double shear pulling tests, the expression is:

$$F_{max} = b_f \sqrt{2 \cdot E_f \cdot t_f \cdot G \cdot (1+\lambda)} \qquad (4)$$

Täljsten (1996) showed that by using NLFM (Nonlinear Fracture Mechanics) Equation (4) is also valid for common civil engineering applications, in which the epoxy adhesives are used to apply the FRP reinforcement.

2.2 *Existing design models*

In the single or double shear pulling test, the most common failure mechanism starts and propagates a few millimeters beneath the interface FRP-matrix.

The thickness of the matrix involved in the failure mechanism depends on the epoxy resin penetration capability.

The stress approach and the fracture mechanics approach propose determining the property of the interface through the maximum bond stress τ and the fracture energy G, respectively. In present-day applications the identification of these parameters is very difficult, especially for existing structural elements. For this reason, the proposed models correlate the properties of the interface to those of the matrix, as compressive and tensile strengths.

Some significant design formulae will now be mentioned and the involved quantities are expressed in Newtons for loads, millimeters for lengths and MPa for stress values.

Van Germet (1980) and Brosen & van Germet (1997), assuming a triangular shear stress distribution in the bond length of the reinforcement, proposed the following design formula to predict the bond strength of FRP glued on concrete members:

$$F_{max} = 0.5 \cdot b_f \cdot l_b \cdot f_{ctm} \tag{5}$$

where l_b = length of the FRP and f_{ctm} = mean value of concrete tensile strength. The only parameter is the concrete tensile strength f_{ctm}. Nevertheless, this formula does not take into account the strength reserve after first cracking and the concept of transfer length is neglected.

Monti et al. (2003), starting from van Germet's assumptions, proposed a new formula to predict the bond strength and the bond transfer length. In Monti's design model, a bilinear bond stress-slip law is assumed and the relationship found by Brosen & van Germet (1997) is used to identify the variables of the local bond law. The maximum load F for a length lower than the minimum transfer length is:

$$F = F_{max} \cdot \sin\frac{\pi \cdot l_b}{2 \cdot l_{b,max}} \tag{6}$$

where

$$F_{max} = 1.41 \cdot k_b \cdot b_f \sqrt{E_f \cdot t_f \cdot f_{ctm} \cdot c_f} \tag{7a}$$

and $l_{b,max}$ = minimum transfer length of FRP expressed as:

$$l_{b,max} = \sqrt{\frac{E_f \cdot t_f}{\sqrt{7.2 \cdot k_b \cdot f_{ctm}}}} \tag{7b}$$

In Equations (7a) and (7b), k_b is a size factor:

$$k_b = \sqrt{1.5\frac{\left(2 - \frac{b_f}{b}\right)}{\left(1 + \frac{b_f}{100mm}\right)}} \tag{7c}$$

where b = width of the reinforced element surface and c_f = 0.3 mm.

Holzenkämpfer (1994) investigated the bond strength between steel plate and concrete by using the NLFM approach. The modified form, in which the reinforcing material consists of FRP, presented by Niedermeier (1996) earlier, and Neubauer & Rostásy (1997) after, has been adopted in the fib CEB-FIP guidelines (2001) for concrete structures as follows:

$$F = F_{max} \frac{l_b}{l_{b,max}}\left(2 - \frac{l_b}{l_{b,max}}\right) \tag{8}$$

where

$$F_{max} = \alpha \cdot c_1 \cdot k_c \cdot k_b \cdot b_f \sqrt{E_f \cdot t_f \cdot f_{ctm}} \tag{9a}$$

$$l_{b,max} = \sqrt{\frac{E_f \cdot t_f}{c_2 \cdot f_{ctm}}} \tag{9b}$$

$$k_b = 1.06\sqrt{\frac{2 - \frac{b_f}{b}}{1 + \frac{b_f}{400mm}}} \tag{9c}$$

in which α = reduction factor to take into account the influence of the inclined cracks on the bond strength; c_1 and c_2 = free parameters to calibrate the bond tests and k_c = factor accounting for the state of compaction of the concrete.

The model proposed by Chen & Teng (2001) is based on experimental test data available in the literature and assumes, as the parameter characteristic of the matrix, compressive strength instead of the tensile strength of the matrix. The maximum load F for a length lower than the minimum transfer length is also expressed as in Equation (6), in which

$$F_{max} = 0.427 \cdot k_b b_f \sqrt{E_f \cdot t_f \sqrt{f'_c}} \tag{10a}$$

$$l_{b,max} = \sqrt{\frac{E_f \cdot t_f}{\sqrt{f'_c}}} \tag{10b}$$

$$k_b = \sqrt{\frac{\left(2 - \frac{b_f}{b}\right)}{\left(1 + \frac{b_f}{b}\right)}} \qquad (10c)$$

where f'_c = cylindrical compressive strength of the concrete.

3 EXPERIMENTAL INVESTIGATION

The experimental investigation, based on double shear pulling tests is addressed to recording the load-carrying capacity and to estimate the effective transfer length for specimens prepared with CFRP sheets bonded to natural stone. In Fig. 1 the specimens prepared with three different bond lengths are shown.

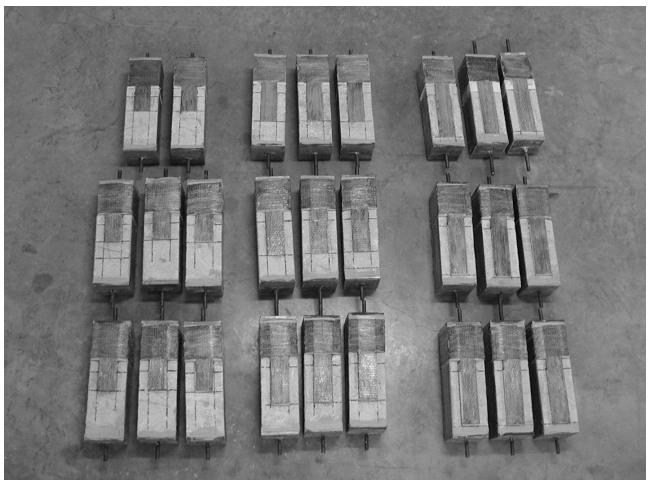

Figure 1. Specimens

3.1 *Specimens*

The consecutive preparation phases of the specimens are shown in Fig. 2.

The specimen consists of two calcarenite natural stone prisms of dimensions quoted in Fig. 2; at the ends of the prisms a square steel plate is connected to a steel rod inserted in a hole. The prisms are only connected through the carbon fiber reinforcing polymer sheets.

The mechanical properties of the calcarenite were deduced by means of compressive tests on cubic specimens and indirect bending tensile tests on prismatic specimens; the specimens were extracted from the same ashlars used for the bond tests. The mean values obtained were f_b = 3.37 MPa and $f_{bt,fl}$ = 0.48 MPa respectively. The FRP sheet consisted of carbon fiber impregnated with epoxy resin; the properties of the fibers obtained from the manufacturer are the following: thickness t_f = 0.13 mm; Young's modulus E_f = 230 GPa and the ultimate tensile strength f_f =3500 MPa.

CFRP sheets were bonded at two opposite sides of the specimen and the cubic calcarenite ashlar was wrapped with a confining CFRP, allowing the occurrence of delamination only on the prismatic specimens.

Nine specimens were prepared for each bond length: 50 mm, 100 mm and 150 mm. For all specimens the same width of CFRP sheet was used, because the investigation was addressed to estimating the effective bond length, i.e. the length along which the stress transfer occurs. The width of the sheet exhibited great influence on the bond behavior only when it was less than 10 mm (Nakaba et al. 1999).

3.2 *Loading and measurement*

Each specimen was set in a universal testing machine with maximum capacity equal to 600 kN and submit-

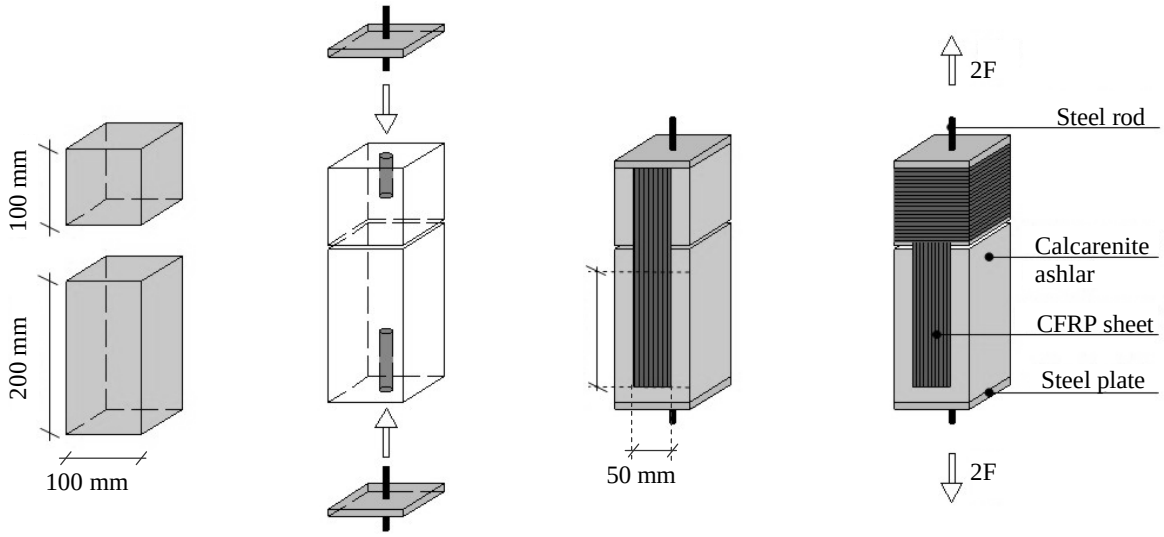

Figure 2. Sequences of preparation specimens

ted to pure tensile force through steel rods, causing direct shear to be placed on the CFRP sheets. Spherical joints were placed at the top and the bottom grips in order to avoid any bending moment caused by eccentricity. For some specimens, in addition to the maximum load-carrying capacity, the total displacement at the section in which the tensile force was applied was measured at each load step by using a linear variable displacement transducer (two LVDTs, one for each side) and the strain distribution

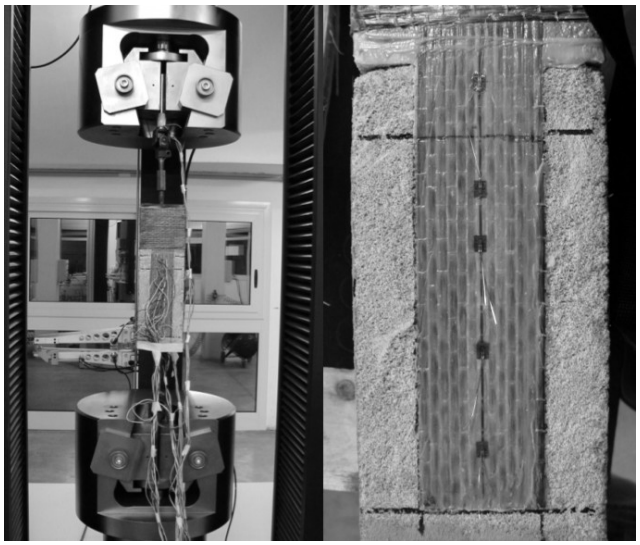

Figure 3. Testing machine and strain-gauge position.

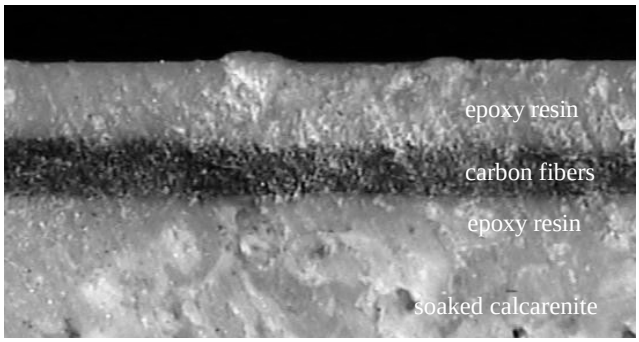

Figure 4. CFRP-calcarenite interface.

was obtained from five strain-gauges (HBM model LY11 – 1.5/120Ω) set on the CFRP sheet (ten strain-gauges were placed on both opposite sides). The measures reported in the next section refer to the side on which the failure mechanism took place. All the quantities measured (forces, displacements and strains) were recorded by HBM MGC plus data acquisition system with 16 channels. The testing machine and the position of the strain-gauges on a side are shown in Fig. 3.

3.3 *Results*

All the specimens were submitted to tensile force until total failure of the bond took place. The typical failure started and propagated inside the calcarenite block until total debonding of the reinforcement occurred. The thickness torn off the calcarenite block was estimated to be approximately between 2 ÷ 4 mm, depending on epoxy resin penetration capability (see Fig. 4). In Table 1, for three different bond lengths, the following quantities are shown: - the numbering of the specimens; - half the maximum external loads recorded; - the cubic compressive strength of the calcarenite obtained by specimens extracted from the ashlars at the end of the tests.

In Fig. 5 the load-slip curves for four tests are plotted; the slip δ between calcarenite stone and CFRP sheet is relative to the loaded end.

Two curves refer to specimens with bond length L= 150mm and two curves to specimens with L= 100mm.The slips were obtained from the LVDT located on the side where the failure took place.

The tests with different bond length revealed similar behavior; they showed linear behavior up to (0.75 ÷ 0.85) F_{max}, followed by nonlinear behavior until debonding took place. As is known, when debonding starts, it moves along the bond length of the reinforcement until total failure occurs. The sub-horizontal branch of the curves represents this phenomenon.

The curves in Fig. 5 show a similar pattern characterized by a sub-horizontal branch after elastic behavior. This reveals that the bond length (150 mm

Table 1. Test results.

Specimen L=150mm	F_{max} (kN)	f_b (N/mm^2)	Specimen L=100mm	F_{max} (kN)	f_b (N/mm^2)	Specimen L=50mm	F_{max} (kN)	f_b (N/mm^2)
1	5.04	3.73	10	4.93	4.24	19	2.28	3.02
2	3.92	2.33	11	4.25	2.89	20	2.31	3.91
3	4.66	2.17	12	4.43	3.43	21	4.73	6.52
4	4.28	2.87	13	4.61	3.83	22	2.22	2.98
5	4.73	4.13	14	4.07	3.17	23	2.33	3.24
6	4.83	4.37	15	3.28	3.58	24	2.20	3.35
7	3.89	3.50	16	4.65	3.65	25	2.13	4.15
8	4.01	3.53	17	3.35	3.31	26	3.51	2.82
9	4.20	2.92	18	----	----	27	----	----

and 100 mm) used for these tests was longer than the minimum transfer length. Furthermore, the curves with L = 100 mm have a lower ultimate slip value than the tests with bond length L = 150 mm, in agreement with debonding propagation.

In Fig. 6 data recorded from the strain-gauges placed on CFRP sheets for both the sides of double shear pulling tests are reported, for specimen 11 with bond length L = 100 mm (Fig. 6a) and for specimen 2 with L = 150 mm (Fig. 6b). Each strain profile is plotted for a given load level. Comparison between the profiles on the sides of the same test shows symmetric strains in the load range in which the local bond stress-slip behavior at the interface is linear, as stressed in a previous investigation carried out by the same authors (Accardi et al. 2003). After that, the damage starts on one of the two sides and it propagates until total failure occurs. This is in agreement with considering half the external load as the maximum load in Table1.

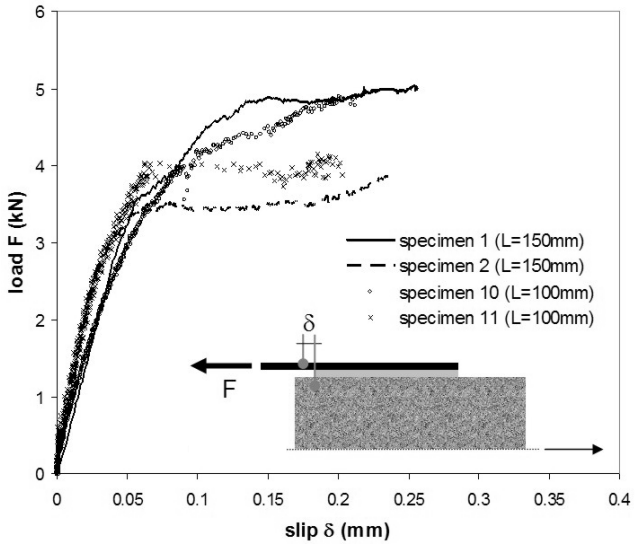

Figure 5. Load-slip curves.

In the range in which the bond stress-slip relationship is linear, the strain distribution, for both tests reported in Fig. 6, follows an exponential decay from the loaded end to a length between 40 and 80 mm. When the load increases, the curves change shape until they change their concavity. The transition phase between the elastic range and the beginning of debonding is characterized by softening behavior of the bond stress-slip law at the interface (Accardi et al. 2003).

Complete debonding of the joint starts when the recorded values of two consecutive strain-gauges become almost equal (Fig. 6b). The length of the portion between the debonding section and the section with zero strain represents the minimum transfer length $l_{b,max}$. After this stage, the load is almost constant but the debonding increases shifting the minimum transfer length until the CFRP sheet has completely peeled from the matrix.

It is possible to observe that both results in Figs. 5 and 6 lead to the consideration that $l_{b,max}$ is less than the bond length used for the two tests but the shift is more evident for the bond length L=150mm.

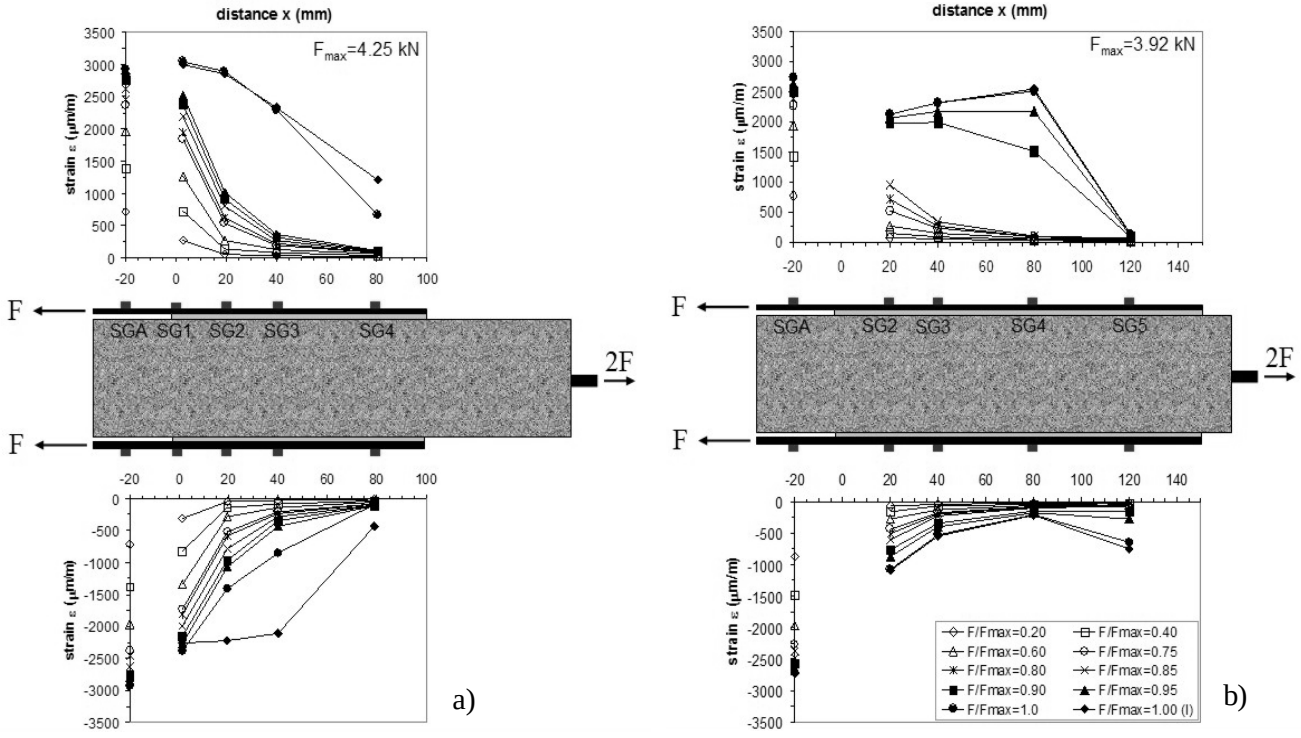

Figure 6. Strain profile along the length of the CFRP sheet a) specimen 11 (L = 100mm); b) specimen 2 (L = 150mm)

4 COMPARISON WITH DESIGN PROPOSALS

The design formulae presented in section 2, validated to predict the bond between concrete-FRP, are used here to compare the experimental results obtained in this investigation carried out on double shear pulling tests to characterize the bond between calcarenite stone and CFRP. In order to make the experimental results comparable with the previously mentioned design formulae, it is necessary to convert the tensile strength and the cylindrical compressive strength (Italian Code, D.M. 09.01.96, LL.PP.): the tensile strength f_{ctm}, used in Equations (7) and (9), is multiplied by 1.2 in order to obtain the indirect bending tensile strength; the cylindrical compressive strength f'_c, used in Equations (10), is divided by 0.83 to obtain the cubic compressive strength.

The modified design formulae lead to the curves plotted in Fig. 7, in which the average parameters (f_b = 3.37 MPa and $f_{bt,fl}$ = 0.48 MPa) are adopted for the tests in the present investigation. The results relative to specimen 21 were excluded from the experimental data because they are very different from all the others. In the same diagram the experimental values for the tests shown in Table 1 are also given.

The curve based on Chen & Teng (2001) fit better than the other curves. This is probably correlated to the determination of the strength parameters chosen to characterize heterogeneous materials like calcarenite stone: tensile strength is more sensitive to imperfections inside the materials than compressive strength. Nevertheless, it is important to notice that both curves using the tensile strength parameter reveal different behavior.

The effectiveness and higher usability of Chen & Teng's model due to the use of compressive strength is further investigated in Fig. 8. The two curves are plotted using the lower and upper cubic compressive strengths shown in Table1 and the experimental results reported in the same diagram are in agreement with the defined limits.

In Fig. 9 the maximum load based on Equations (10) is also shown in the variation of the compressive strength. This expression, validated on concrete materials, has been extended to materials like that used here.

The curve for materials with low cubic compressive strength (less than 15 MPa) fits with good approximation the experimental results obtained in this and in a previous investigation for tests with a bond length larger than the minimum transfer length (Failla et al. 2002).

Therefore, Equations (6) and (10), for the data available, seem to predict the bond strength of calcarenite-CFRP joints and the most important parameter is the cubic compressive strength of the materials on which the reinforcement is glued.

Moreover, in order to make a more adequate evaluation of $l_{b,max}$ by using the analytical models considered here, it is necessary to test more specimens to obtain a good calibration of the parameters that are present in the formulae.

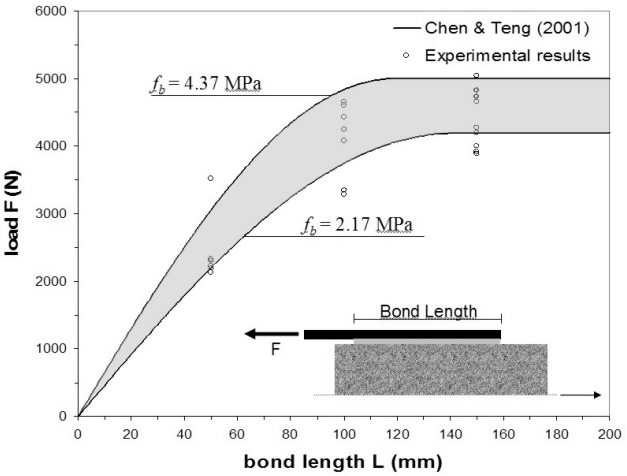

Figure 8. Range defined by analytical model and comparison with experimental results.

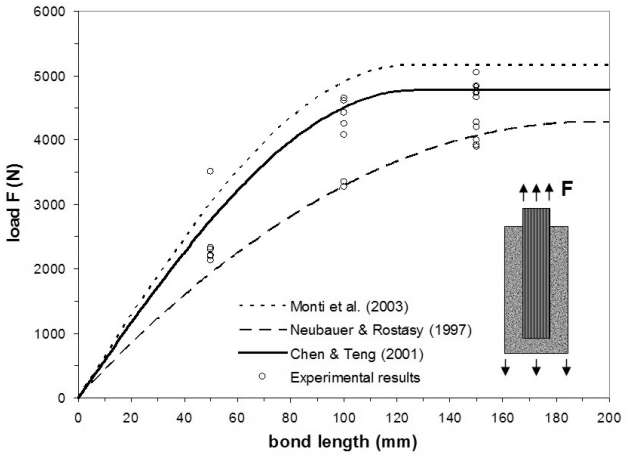

Figure 7. Comparison between different analytical models and experimental results.

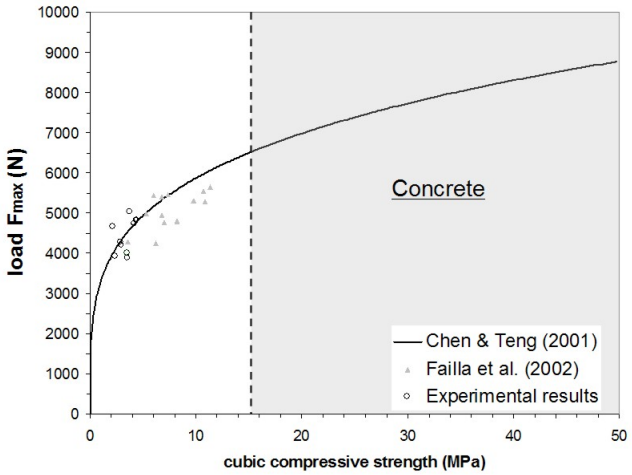

Figure 9. Curve fitting experimental results.

5 CONCLUSIONS

Double shear pulling tests were adopted to evaluate some of the parameters affecting the FRP to calcarenite stone bond. Failure occurred in the calcarenite block a few millimeters beneath the calcarenite-epoxy resin interface. Due to the failure mode, the calcarenite strength affects the maximum load. Therefore, the existing bond models, used for concrete strengthening with FRP, are extended to predict the maximum load and minimum transfer length for calcarenite stone.

Comparison with the experimental results shows that the model by Chen & Teng (2001) is more effective and very easy to use to predict the bond parameters for this kind of natural stone.

Furthermore, the low cubic compressive strength of the calcarenite stone used in this investigation reveals the possibility of extending the application of the same model to other materials like these.

The design of FRP strengthened masonry members can follow the principles of conventional reinforced masonry design as reported in Triantafillou (1988), but the bond anchorage requires particular attention. For this reason it is appropriate to take another ultimate state limit into account for debonding.

In order to evaluate the proper ultimate condition of structural masonry element sections, subjected to axial load and bending moment, it is possible to deduce the ultimate strain for the FRP reinforcement from the bond strength for the joint as pointed out in this investigation.

REFERENCES

Accardi, M., La Mendola L. & Zingone G. 2004. CFRP sheets bonded to natural stone: interfacial phenomena. *Damage and Fracture Mechanics VIII, Computer Aided Assessment and Control*. Crete, Greece, pp. 173 -182.

Brosens, K. & van Gemert, D. 1997. ''Anchoring stresses between concrete and carbon fibre reinforced laminates.'' *Non-Metallic (FRP) Reinforcement for Concrete Struct., Proc., 3rd Int. Symp., Japan Concrete Institute*, Sapporo, 1: 271–278.

Chen J. F. & Teng J. G. 2001. Anchorage strength models for FRP and steel plates bonded to concrete. *Journal of Structural Engineering*, 127(7).

Como, M., Iannіruberto, U. & Imbimbo, M. 2000. La resistenza degli archi murari rinforzati con fogli in FRP. *Proc. Of Mechanics of masonry structures strengthned with FRP materials*, Venezia, Italy.

Ehsani, M.R., Saadatmanesh, H. & Velazques-Dimas, J.I. 1999. Behaviour of retrofitted URM walls under simulated earthquake loadind. *Journal of Composite for Construction*, ASCE 3(3): 134-142.

Failla, A., Accardi, M., Rizzo, G., Algozzini, G., Pellitteri, G. & Buscaglia, G. 2002. The use of CFRPs in strengthening of historical masonry structures: investigation on durability by accelerated testing. *Durability of fiber reinforced polymer (FRP) composites for construction*, Montreal. May 29 –31: 297-303.

Faccio, P. & Foraboschi, P. 2000. Experimental and theoretical analysis of masonry vaults with FRP reinforcementes. *3° International Conference on Advanced Composite Materials in Bridges and Structures*, Ottawa, Canada:629-636.

fib CEB-FIP. 2001, "Externally bonded FRP reinforcement for RC structures. Bulletin 14. Technical Report on the Design and use of externally bonded fibre reinforced polymer reinforcement (FRP EBR) for reinforced concrete structures". Task Group 9.3.

Holzenkämpfer, P. 1994. Ingenieurmodelle des Verbunds geklebter Bewehrung für Betonbauteile. *Ph.D. thesis*, TU Braunschweig.

Horiguchi, T. & Saeki, N. 1997. Effect of test methods and quality of concrete on bond strength of CFRP sheet. *Non-Metallic (FRP) Reinforcement for Concrete Struct ., Proc., 3rd Int. Symp., Japan Concrete Institute*. Sapporo, 1: 475–482.

Luciano, R. & Sacco E. 1998. Famage of masonry panels reinforced by FRP sheets. *International Journal of Solids and Structures* 35: 1723-1741.

Monti, G., Renzelli, M. & Luciani, P. 2003. FRP adhesion in uncracked and cracked concrete zones. *Proc. Sixth Int. Symposium on FRP Reinforcement for Concrete Structures (FRPRCS-6)*, Singapore, Japan.

Nakaba, K., Kanakubo T., Furuta, T. & Yoshizawa H. 2001. Bond Behavior between fiber-reinforced polymer laminates and concrete. *ACI Structural Journal*, 98(3) : 359-367.

Neubauer, U. & Rostásy, F. S. 1997. Design aspects of concrete structures strengthened with externally bonded CFRP plates. *Proc.,7th Int. Conf. on Struct. Faults and Repairs*, ECS Publications, Edinburgh, Scotland, 2: 109–118.

Niedermeier, R. 1996. Stellungnanme zur Richtlinie für das Verkleben von Betonbauteilen durch Ankleben von Stahllaschen-Entwurf März. *Schreiben 1390 vom 30.10.1996 des Lehrstuhls für Massivbau*, Technische Universität München, Germany.

Ottosen, N.S. & Olsson, K.G. 1988. Hardening/Softening Plastic Analysis of Adhesive Joints. *Journal Engineering Mechanics* 114(1): 97-116.

Pichler D. 1993. Die Wirkung von Anpressdrücken auf die Verankerung von Klebelamellen. *Ph.D. thesis*, Leopold-Franzens-Universität Innsbruck.

Triantafillou, T. C. 1998. Strengthening of Masonry Structures using Epoxy-Bonded FRP Laminates. *Journal of Composites for Construction*, 2 (2).

Taljsten, B. 1996. Strengthening of concrete prisms using the plate – bonding technique. *International Journal of Fracture*. No. 82.

Valluzzi, M.R., Valdemarca, M. & Modena, C. 2001. Behavior of brick masonry vaults by FRP laminates. *Journal of Composites for Construction*, ASCE: 163-169.

Van Gemert, D. 1980. Force transfer in epoxy-bonded steel-concrete joints. *Int. J. Adhesion and Adhesives*, 1: 67-72.

Volkersen, O. 1938: Die Nietkrafverteilung in zugbeanspruchten Nietverbindungen mit konstanten Laschenquerschnitten. *Ph.D. thesis, Luftfahrtforschung*, 15, pp. 41-47.

Wu, Z., Yuan, H. & Niu, H. 2002. Stress transfer and fracture propagation in different kinds of adhesive joints. Journal of Engineering Mechanics, ASCE, 128(5): 562-573.